PERGAMON

International Journal of Solids and Structures 38 (2001) 9461–9478

INTERNATIONAL JOURNAL OF SOLIDS and STRUCTURES

www.elsevier.com/locate/ijsolstr

Modeling and numerical issues in hyperelasto-plasticity with anisotropy

Magnus Ekh *, Kenneth Runesson

Department of Solid Mechanics, Chalmers University of Technology, M-huset, Horslsvagen 7, SE-41296 Göteborg, Sweden

Received 27 October 1999; in revised form 23 June 2000

Abstract

In the paper we discuss modeling and numerical issues that arise in conjunction with anisotropic hyperelastic–plastic response. Both elastic and plastic anisotropy are included. A particular kinematic hardening rule is proposed and its predictive capability is investigated. From the numerical viewpoint, we are concerned with the algorithmic consequences of the loss of coaxiality that arises from anisotropy. The numerical investigation shows that significant truncation errors are introduced if commonly used linearizations of the (classical) exponential Backward Euler rule are utilized in the presence of non-coaxiality. © 2001 Published by Elsevier Science Ltd.

Keywords: Plasticity; Anisotropy; Large strains

1. Introduction

Within the context of large strain plasticity and viscoplasticity, the classical concept of multiplicative split of the deformation gradient has won widespread acceptance in the computational mechanics community in recent years. This concept gives rise to an evolution law for the plastic part of the deformation gradient as part of an associative structure, that emanates from the particular form of the dissipation inequality. The situation is far less clear for the corresponding evolution equations pertinent to the internal variables that represent hardening. This ambiguity is particularly pronounced for kinematic hardening, which is an issue that has attracted considerable attention in recent years (e.g. Eterovic and Bathe, 1990; Schieck and Stumpf, 1995; Tsakmakis, 1996; Svendsen et al., 1998; Münz et al., 1999). Ideally, a number of requirements should be met by the model in order to become acceptable: (1) Physically sound behavior must be represented, e.g. the pathological oscillations of shear stresses in simple shear, shown by certain hypoelasticity-based models employing the Jaumann stress rate, cannot be accepted. (In fact, such behavior is obtained even for hyperelasticity-based models with the inappropriate choice of hardening rules; cf. below.) (2) The model should be thermodynamically consistent, i.e. the dissipation inequality should be satisfied. (3) The back-stress should preserve symmetry in the spatial format. As it turns out (see also discussion later), it seems difficult to

* Corresponding author.
E-mail address: mekh@solid.chalmers.se (M. Ekh).

0020-7683/01/$ - see front matter
PII: S0020-7683(01)00132-9

satisfy the requirements (2) and (3) simultaneously, at least for the class of models discussed in this paper and most models proposed in the literature.

Kinematic hardening is anisotropic in the sense that the yield surface can no longer be expressed as an isotropic function of the stress tensor, and the consequence is that coaxiality between the elastic deformation and the (Mandel type) back-stress is lost. If we also include hyperelastic anisotropy into the formulation, then this will lead to the loss of coaxiality between the elastic deformation and the (Mandel) stress itself. Furthermore, the Mandel stress on the intermediate configuration will be non-symmetrical in general. The loss of coaxiality between the different deformation and stress measures, regardless of the source, is of importance for the proper algorithmic implementation of the rule used for integrating the evolution equations of the internal variables, in particular the flow rule. In this paper we shall employ the classical (exponential) Backward Euler rule. In particular, when the logarithmic hyperelastic law, Weber and Anand (1990), is used, then it is common to exploit the logarithm rules for products of coaxial tensors in order to achieve an incremental format that becomes virtually identical to that of small strain theory of plasticity. Although such an algorithm is still consistent (at least first order accurate) in the presence of non-coaxiality, it may produce truncation errors of significant magnitude. A prime purpose of this paper is to investigate this issue by way of comparing the "truly nonlinear" algorithm with another algorithm that is based on an appealing linearization.

The paper is organized as follows: after some preliminary remarks on large deformation kinematics, we propose the hyperelastic-plastic framework with kinematic hardening in Section 2. As part of the prototype model, we choose a transversely isotropic elasticity law that is linear in terms of the logarithmic strains. Mixed nonlinear hardening of the Armstrong–Frederick type is chosen; in particular employing the "plastic-rotation-neutralized" (PRN) format, which is described in some detail. In Section 3, we give the incremental format of the constitutive relations. The "exact" and properly "linearized" formulations are outlined. It is also discussed how to compute the algorithmic tangent stiffness (ATS) tensor from the "local" incremental problem for a given deformation increment. Finally, we present a series of numerical results for the (homogeneous) simple shear mode, as well as for the unconstrained shear problem. The latter problem represents a non-homogeneous deformation state and, therefore, requires finite element analysis.

2. Thermodynamics and constitutive relations

2.1. Preliminaries on the kinematics

The main kinematic assumption is the classical multiplicative split of the deformation gradient $\boldsymbol{F} = \bar{\boldsymbol{F}} \cdot \boldsymbol{F}^{\mathrm{p}}$, where $\boldsymbol{F}^{\mathrm{p}}$ is the deformation from the initial configuration Ω_0 [1] to the "intermediate" or "inelastic" configuration $\bar{\Omega}$, whereas $\bar{\boldsymbol{F}}$ represents the elastic deformation from $\bar{\Omega}$ to the current configuration Ω. Moreover, we consider an auxiliary reference configuration Ω_{ref}, from which $\bar{\Omega}$ can be reached via a push-forward with the deformation gradient $\boldsymbol{F}^{\mathrm{p}}_{\mathrm{ref}}$, cf. Fig. 1. The role of this auxiliary configuration will be explained in the context of kinematic hardening (as discussed later). Depending on the choice of Ω_{ref}, different "neutralized" formats are possible:

- Plastic deformation neutralized (PDN) format, defined by $\Omega_{\mathrm{ref}} = \Omega_0$ ($\boldsymbol{F}^{\mathrm{p}}_{\mathrm{ref}} = \boldsymbol{F}^{\mathrm{p}}$).
- PRN format, defined by $\Omega_{\mathrm{ref}} = \Omega_{\mathrm{PRN}}$ ($\boldsymbol{F}^{\mathrm{p}}_{\mathrm{ref}} = \boldsymbol{R}^{\mathrm{p}}$ with $\boldsymbol{R}^{\mathrm{p}} = \boldsymbol{F}^{\mathrm{p}} \cdot (\boldsymbol{U}^{\mathrm{p}})^{-1}$).
- Unrotated (UR) format, defined by $\Omega_{\mathrm{ref}} = \bar{\Omega}$ ($\boldsymbol{F}^{\mathrm{p}}_{\mathrm{ref}} = \boldsymbol{\delta}$).

[1] Ω_0 is taken as the "computational domain" throughout.

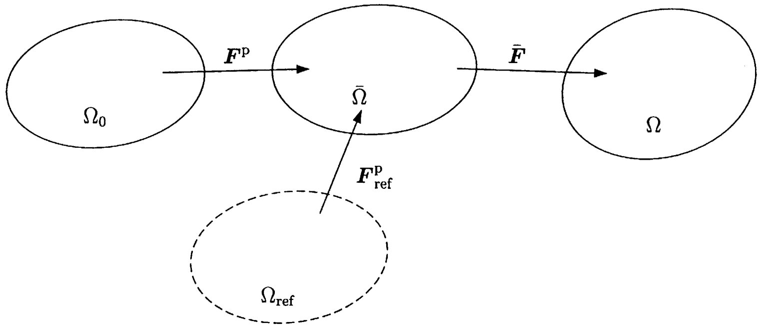

Fig. 1. Kinematic transformations involved in hyperelasto-(visco) plasticity with kinematic hardening.

The (right) deformation tensors $\boldsymbol{C}$ and $\bar{\boldsymbol{C}}$, associated with Ω_0 and $\bar{\Omega}$, respectively, are obtained via the usual (covariant) pull-back of $\boldsymbol{\delta}$ from Ω:

$$\boldsymbol{C} = \boldsymbol{F}^{\mathrm{T}} \cdot \boldsymbol{F} = (\boldsymbol{F}^{\mathrm{p}})^{\mathrm{T}} \cdot \bar{\boldsymbol{C}} \cdot \boldsymbol{F}^{\mathrm{p}}, \quad \bar{\boldsymbol{C}} = \bar{\boldsymbol{F}}^{\mathrm{T}} \cdot \bar{\boldsymbol{F}} \tag{1}$$

Henceforth, $\bar{\boldsymbol{C}}$ is denoted the "elastic deformation". Correspondingly, the second Piola–Kirchhoff (PK) stress tensors $\boldsymbol{S}_2$ and $\bar{\boldsymbol{S}}_2$, associated with Ω_0 and $\bar{\Omega}$, are obtained via the usual (contravariant) pull-back of the Kirchhoff stress $\boldsymbol{\tau}$ from Ω:

$$\boldsymbol{S}_2 = \boldsymbol{F}^{-1} \cdot \boldsymbol{\tau} \cdot \boldsymbol{F}^{-\mathrm{T}} = (\boldsymbol{F}^{\mathrm{p}})^{-1} \cdot \bar{\boldsymbol{S}}_2 \cdot (\boldsymbol{F}^{\mathrm{p}})^{-\mathrm{T}}, \quad \bar{\boldsymbol{S}}_2 = \bar{\boldsymbol{F}}^{-1} \cdot \boldsymbol{\tau} \cdot \bar{\boldsymbol{F}}^{-\mathrm{T}} \tag{2}$$

We also introduce the Mandel stress tensors $\boldsymbol{T}$ and $\bar{\boldsymbol{T}}$ on Ω_0 and $\bar{\Omega}$, respectively, as:

$$\boldsymbol{T} = \boldsymbol{C} \cdot \boldsymbol{S}_2 = \boldsymbol{F}^{\mathrm{T}} \cdot \boldsymbol{\tau} \cdot \boldsymbol{F}^{-\mathrm{T}} = (\boldsymbol{F}^{\mathrm{p}})^{\mathrm{T}} \cdot \bar{\boldsymbol{T}} \cdot (\boldsymbol{F}^{\mathrm{p}})^{-\mathrm{T}}, \quad \bar{\boldsymbol{T}} = \bar{\boldsymbol{F}}^{\mathrm{T}} \cdot \boldsymbol{\tau} \cdot \bar{\boldsymbol{F}}^{-\mathrm{T}} = \bar{\boldsymbol{C}} \cdot \bar{\boldsymbol{S}}_2 \tag{3}$$

Finally, we introduce the right and left elastic stretch tensors $\bar{\boldsymbol{U}}$ and $\boldsymbol{v}^{\mathrm{e}}$ and $\bar{\Omega}$ and Ω, respectively, from the decompositions $\bar{\boldsymbol{F}} = \bar{\boldsymbol{R}} \cdot \bar{\boldsymbol{U}} = \boldsymbol{v}^{\mathrm{e}} \cdot \bar{\boldsymbol{R}}$, where $\bar{\boldsymbol{R}}$ is the rotation involved in $\bar{\boldsymbol{F}}$.

Remark. In the case that $\boldsymbol{\tau}$ is governed by an *isotropic* hyperelastic law, then $\boldsymbol{\tau}$ and $\boldsymbol{v}^{\mathrm{e}}$ commute, and it follows that $\bar{\boldsymbol{T}} = \boldsymbol{\tau}^{\mathrm{ERN}}$, where $\boldsymbol{\tau}^{\mathrm{ERN}}$ is the "elastic-rotation-neutralized" version of $\boldsymbol{\tau}$, defined as

$$\boldsymbol{\tau}^{\mathrm{ERN}} = \bar{\boldsymbol{R}}^{\mathrm{T}} \cdot \boldsymbol{\tau} \cdot \bar{\boldsymbol{R}} \tag{4}$$

Although $\bar{\boldsymbol{T}}$ is symmetrical in this case, $\boldsymbol{T}$ may still be non-symmetrical (in general).

We may also perform a pull-back of $\bar{\boldsymbol{T}}$ to Ω_{ref} to obtain

$$\boldsymbol{T}_{\mathrm{ref}} = (\boldsymbol{F}^{\mathrm{p}}_{\mathrm{ref}})^{\mathrm{T}} \cdot \bar{\boldsymbol{T}} \cdot (\boldsymbol{F}^{\mathrm{p}}_{\mathrm{ref}})^{-\mathrm{T}} \tag{5}$$

which is (in general) a non-symmetric tensor even if $\bar{\boldsymbol{T}}$ is symmetrical.

2.2. Hyperelastic–plastic model framework with kinematic hardening

Subsequently, we shall consider combined kinematic and isotropic hardening under isothermal conditions. In analogy with the approach adopted for kinematically linear theory, we then introduce the free energy $\Psi(\bar{\boldsymbol{C}}, \bar{\boldsymbol{\beta}}, \bar{\kappa})$ in terms of tensorial quantities defined on $\bar{\Omega}$ (measured per unit volume of the computational domain Ω_0). Here, we introduced the second order tensor $\bar{\boldsymbol{\beta}}$ as a "strain-like" variables (defined on $\bar{\Omega}$) that represents kinematic hardening, whereas $\bar{\kappa}$ is a scalar that represents isotropic hardening.

From the second law of thermodynamics, we obtain in standard fashion the elastic law and the dissipation inequality, which can be expressed as

$$\bar{\boldsymbol{S}}_2 = 2\frac{\partial \Psi}{\partial \bar{\boldsymbol{C}}}, \quad D \stackrel{\text{def}}{=} \bar{\boldsymbol{T}} : \bar{\boldsymbol{L}}^{\text{p}} + \bar{\boldsymbol{B}} : \dot{\bar{\boldsymbol{\beta}}} + \bar{K}\dot{\bar{\kappa}} \geqslant 0, \quad \bar{\boldsymbol{T}} : \bar{\boldsymbol{L}}^{\text{p}} = \bar{\boldsymbol{T}}^{\text{sym}} : \bar{\boldsymbol{D}}^{\text{p}} + \bar{\boldsymbol{T}}^{\text{skw}} : \bar{\boldsymbol{W}}^{\text{p}} \tag{6}$$

where $\bar{\boldsymbol{L}}^{\text{p}} \stackrel{\text{def}}{=} \dot{\mathbf{F}}^p \cdot (\boldsymbol{F}^{\text{p}})^{-1}$ is the "material plastic strain velocity" on $\bar{\Omega}$, $\bar{\boldsymbol{D}}^{\text{p}} \stackrel{\text{def}}{=} (\bar{\boldsymbol{L}}^{\text{p}})^{\text{sym}}$ is the rate of plastic deformation and $\bar{\boldsymbol{W}}^{\text{p}} \stackrel{\text{def}}{=} (\bar{\boldsymbol{L}}^{\text{p}})^{\text{skw}}$ is the plastic spin.

Remark. Whenever $\bar{\boldsymbol{T}}$ is symmetrical (such as for isotropic elasticity), it appears that $\bar{\boldsymbol{W}}^{\text{p}}$ does not affect the dissipation and, thus, has no thermodynamic relevance.

Moreover, $\bar{\boldsymbol{B}}$ and $\bar{K}$ are the "backstress" and "dragstress" respectively, defined as

$$\bar{\boldsymbol{B}} = -\frac{\partial \Psi}{\partial \bar{\boldsymbol{\beta}}}, \quad \bar{K} = -\frac{\partial \Psi}{\partial \bar{\kappa}} \tag{7}$$

By a push-forward of $\bar{\boldsymbol{B}}$ to the current configuration Ω, we obtain the corresponding back-stress $\boldsymbol{b}$ of the "Kirchhoff type":

$$\boldsymbol{b} = \bar{\boldsymbol{F}}^{-\text{T}} \cdot \bar{\boldsymbol{B}} \cdot \bar{\boldsymbol{F}}^{\text{T}} \tag{8}$$

Plastically admissible states are now defined by the convex set $\mathscr{B}$:

$$\mathscr{B} = \{\bar{\boldsymbol{T}}, \bar{\boldsymbol{B}}, K | \boldsymbol{\Phi}(\bar{\boldsymbol{T}}^{\text{r}}, K) \leqslant 0\} \tag{9}$$

where $\boldsymbol{\Phi}$ is the yield function and $\bar{\boldsymbol{T}}^{\text{r}} = \bar{\boldsymbol{T}} - \bar{\boldsymbol{B}}$ is the reduced stress. It is noted that $\bar{\boldsymbol{T}}^{\text{r}}$ is non-symmetrical in the general situation.

2.3. Prototype model: transverse elastic anisotropy

Elastic–plastic decoupling will be assumed via an additive decomposition of Ψ into elastic and plastic parts: $\Psi(\bar{\boldsymbol{C}}, \bar{\boldsymbol{\beta}}, \bar{\kappa}) = \Psi^{\text{e}}(\bar{\boldsymbol{C}}) + \psi^{\text{p}}(\bar{\boldsymbol{\beta}}, \bar{\kappa})$. In order for $\Psi^{\text{e}}(\bar{\boldsymbol{C}})$ to represent anisotropic elastic response, we first establish the pertinent relations for orthotropy and then specialize to transverse isotropy. Moreover, we shall express the elasticity relations in terms of the logarithmic elastic strain, defined as $\bar{\boldsymbol{\epsilon}} = \ln(\bar{\boldsymbol{U}}) = \frac{1}{2}\ln(\bar{\boldsymbol{C}})$.

The directions of elastic orthotropy are defined by the orthonormal vectors $\boldsymbol{a}_1, \boldsymbol{a}_2$ and $\boldsymbol{a}_3$, and the corresponding structural tensors are the dyads $\boldsymbol{A}_i = \boldsymbol{a}_i \otimes \boldsymbol{a}_i$ for $i = 1, 2, 3$. According to the representation theorem of a scalar function of two tensors, cf. Spencer (1980), we can now choose the integrity basis for Ψ^{e} in terms of invariants of $\bar{\boldsymbol{\epsilon}}$ and mixed invariants of $\boldsymbol{A}_i \cdot \bar{\boldsymbol{\epsilon}}$. Hence, we define the set of irreducible invariants i_1, i_2 and i_3 of $\bar{\boldsymbol{\epsilon}}$ as

$$i_1 = \boldsymbol{\delta} : \bar{\boldsymbol{\epsilon}}, \quad i_2 = \boldsymbol{\delta} : \bar{\boldsymbol{\epsilon}}^2, \quad i_3 = \boldsymbol{\delta} : \bar{\boldsymbol{\epsilon}}^3 \tag{10}$$

and the set of irreducible invariants $i_{1\mathbf{A}_i}$ and $i_{2\mathbf{A}_i}$ for $i = 1, 2, 3$, as

$$i_{1\mathbf{A}_i} = \boldsymbol{A}_i : \bar{\boldsymbol{\epsilon}}, \quad i_{2\mathbf{A}_i} = \boldsymbol{A}_i : \bar{\boldsymbol{\epsilon}}^2 \tag{11}$$

Now, we consider a form of orthotropic hyperelasticity, which is slightly restricted (as compared to the most general possible) in the sense that the dependence on i_3 is dropped. In this case, it is possible to show that the appropriate integrity basis consists of the six invariants in Eq. (11) such that we use the representation $\Psi(i_{1\mathbf{A}_1}, i_{2\mathbf{A}_1}, i_{1\mathbf{A}_2}, \ldots, i_{2\mathbf{A}_3})$. This format generates a class of elasticity models that contains the most general orthotropic *linear* response at the restriction to small strains.

We now obtain, in particular,

$$\bar{\boldsymbol{T}} = 2\bar{\boldsymbol{C}} \cdot \frac{\mathrm{d}\Psi^{\mathrm{e}}}{\mathrm{d}\bar{\boldsymbol{C}}} = \sum_{i=1}^{3} \left[\frac{\partial \Psi^{\mathrm{e}}}{\partial i_{1\mathbf{A}_i}} \bar{\boldsymbol{C}} \cdot \boldsymbol{A}_i^{\mathrm{ln}} + 2 \frac{\partial \Psi^{\mathrm{e}}}{\partial i_{2\mathbf{A}_i}} \bar{\boldsymbol{C}} \cdot ((\bar{\boldsymbol{\epsilon}} \cdot \boldsymbol{A}_i)^{\mathrm{sym}} : \mathscr{P}^{\mathrm{ln}}) \right] \tag{12}$$

where we introduced the "adjusted" dyads

$$\boldsymbol{A}_i^{\mathrm{ln}} = \boldsymbol{A}_i : \mathscr{P}^{\mathrm{ln}}, \quad \mathscr{P}^{\mathrm{ln}} \stackrel{\mathrm{def}}{=} 2\frac{\mathrm{d}\bar{\boldsymbol{\epsilon}}}{\mathrm{d}\bar{\boldsymbol{C}}} = \frac{\mathrm{d}(\ln(\bar{\boldsymbol{C}}))}{\mathrm{d}\bar{\boldsymbol{C}}} \tag{13}$$

The fourth order transformation tensor $\mathscr{P}^{\mathrm{ln}}$ can be computed in closed-form using the Serrin's formulae (Simo and Taylor, 1991). We remark that $\mathscr{P}^{\mathrm{ln}} \to \mathscr{I}^{\mathrm{sym}}$ for small deformations.

Next, we shall establish an explicit format for $\bar{\boldsymbol{T}}$ such that the response will be linear at small deformation. It can then be shown that Eq. (12) must take the form

$$\bar{\boldsymbol{T}} = \sum_{i=1}^{3} \sum_{j=1}^{3} \Phi_{ij} i_{1\mathbf{A}_j} \bar{\boldsymbol{C}} \cdot \boldsymbol{A}_i^{\mathrm{ln}} + \sum_{i=1}^{3} \Phi_{3+i} \bar{\boldsymbol{C}} \cdot ((\bar{\boldsymbol{\epsilon}}_i \cdot \boldsymbol{A}_i)^{\mathrm{sym}} : \mathscr{P}^{\mathrm{ln}}) \tag{14}$$

where $\Phi_{ij} = \Phi_{ji}$ for $i, j = 1, 2, 3$ and Φ_{3+i} for $i = 1, 2, 3$ are nine constant coefficients to be determined upon orienting the (Cartesian) coordinate system in such a fashion that $\boldsymbol{a}_i$ will coincide with the base vectors. Before doing this, we further simplify matters by introducing transverse isotropy. For convenience, we assume that the plane x_2x_3 is isotropic, whereas the planes x_1x_2 and x_1x_3 are anisotropic with the same properties. This gives $\Phi_{12} = \Phi_{13}$, $\Phi_{22} = \Phi_{23} = \Phi_{33}$, $\Phi_5 = \Phi_6$, which are the five coefficients that can conveniently be expressed in terms of "physical" stiffness coefficients $M_{\parallel}$, $L_{\parallel}$, $G_{\parallel}, L$ and G. Quantities with subindex $\parallel$ refer to planes that contain the preferred direction $(\boldsymbol{a}_1) = \boldsymbol{a}$, whereas quantities without subindex refer to the isotropic plane, that is orthogonal to $\boldsymbol{a}$. To simplify matters even further, we shall subsequently assume that $G_{\parallel} = G$, $L_{\parallel} = L$ and $M_{\parallel} = k(2G + L)$, where k is a scalar factor (and $k = 1$ clearly defines the completely isotropic response). We then obtain

$$\bar{\boldsymbol{T}} = \bar{\boldsymbol{T}}^{\mathrm{iso}} + \bar{\boldsymbol{T}}^{\mathrm{aniso}} \tag{15}$$

where

$$\bar{\boldsymbol{T}}^{\mathrm{iso}} = L i_1 \boldsymbol{\delta} + 2G\bar{\boldsymbol{\epsilon}} = (\mathscr{E}^{\mathrm{e}})^{\mathrm{iso}} : \bar{\boldsymbol{\epsilon}}, \qquad \bar{\boldsymbol{T}}^{\mathrm{aniso}} = (k-1)(2G + L) i_{1\mathbf{A}} \bar{\boldsymbol{C}} \cdot \boldsymbol{A}^{\mathrm{ln}} \tag{16}$$

where $(\mathscr{E}^{\mathrm{e}})^{\mathrm{iso}}$ is the usual constant elastic tangent stiffness tensor for isotropic response at small strains. It appears that $\bar{\boldsymbol{T}}^{\mathrm{iso}}$ is symmetrical, whereas $\bar{\boldsymbol{T}}^{\mathrm{aniso}}$ is non-symmetrical (since $\bar{\boldsymbol{C}}$ and $\boldsymbol{A}^{\mathrm{ln}}$ do not commute in general).

2.4. Prototype model: plastic anisotropy – mixed hardening of metal plasticity

The von Mises yield function, which is expressed in terms of $\bar{\boldsymbol{T}}^{\mathrm{r}}$ (for convenience), including mixed isotropic and kinematic hardening reads

$$\Phi = \bar{T}_{\mathrm{e}}^{\mathrm{r}} - \sigma_y - K \quad \text{with} \quad \bar{T}_{\mathrm{e}}^{\mathrm{r}} = \sqrt{\tfrac{3}{2}} |\bar{\boldsymbol{T}}_{\mathrm{dev}}^{\mathrm{r}}| \tag{17}$$

where $|\boldsymbol{T}| \stackrel{\mathrm{def}}{=} (\boldsymbol{T} : \boldsymbol{T})^{1/2}$ is the norm of the second order tensor $\boldsymbol{T}$. Proposing the plastic part of the free energy in the same way as for small deformations, i.e.

$$\Psi^{\mathrm{p}} = \tfrac{1}{2}(1 - r) H (\bar{\beta}_{\mathrm{e}})^2 + \tfrac{1}{2} r H \kappa^2 \quad \text{with} \quad \bar{\beta}_{\mathrm{e}} = \sqrt{\tfrac{2}{3}} |\bar{\boldsymbol{\beta}}| \tag{18}$$

we obtain the usual hardening stresses, cf. Lemaitre and Chaboche (1990):

$$\bar{\boldsymbol{B}} = -\tfrac{2}{3}(1-r)H\bar{\boldsymbol{\beta}}, \quad \bar{K} = -rH\bar{\kappa} \tag{19}$$

where H is the (uniaxial) hardening modulus and $r \in [0,1]$ is a scalar.

As to the proper choice of the constitutive rate laws for the internal variables, it appears natural to adopt the principle of maximum plastic dissipation from which the dissipation inequality in Eq. (6) would be automatically satisfied. However, there are (at least) two features that call for a modification of this principle: (1) Non-linear hardening of the Armstrong–Frederick type, (2) Replacement of $\dot{\bar{\boldsymbol{\beta}}}$ with a suitable objective rate $\overset{*}{\bar{\boldsymbol{\beta}}}$ with respect to the intermediate configuration $\bar{\Omega}$ in the evolution rule for $\bar{\boldsymbol{\beta}}$. Leaving (for the moment) the crucial issue of how to choose a proper definition of $\overset{*}{\bar{\boldsymbol{\beta}}}$, we propose the evolution rules

$$\bar{\boldsymbol{L}}^{\mathrm{p}} \overset{\mathrm{def}}{=} \dot{\boldsymbol{F}}^{\mathrm{p}} \cdot (\boldsymbol{F}^{\mathrm{p}})^{-1} = \bar{\boldsymbol{D}}^{\mathrm{p}} + \bar{\mathrm{W}}^{\mathrm{p}}, \ \bar{\boldsymbol{D}}^{\mathrm{p}} = \dot{\mu}\bar{\boldsymbol{M}}^{\mathrm{sym}} \quad \text{with} \quad \bar{\boldsymbol{M}} \overset{\mathrm{def}}{=} \frac{\partial \Phi}{\partial \bar{\boldsymbol{T}}} = \frac{3\bar{\boldsymbol{T}}^{\mathrm{r}}_{\mathrm{dev}}}{2\boldsymbol{T}^{\mathrm{r}}_{\mathrm{e}}} \tag{20}$$

$$\overset{*}{\bar{\boldsymbol{\beta}}} = \dot{\mu}(\bar{\boldsymbol{M}}^{*}_{\mathrm{B}})^{\mathrm{sym}} \quad \text{with} \quad \bar{\boldsymbol{M}}^{*}_{\mathrm{B}} = -\left(\bar{\boldsymbol{M}} - \frac{3\bar{\boldsymbol{B}}}{2B_\infty}\right) \tag{21}$$

$$\dot{\kappa} = \dot{\mu}M^{*}_{K} \quad \text{with} \quad M^{*}_{K} = -\left(1 - \frac{K}{K_\infty}\right) \tag{22}$$

where B_∞ and K_∞ are the saturation values of the kinematic and isotropic hardening, respectively.

In the case of plasticity, $\dot{\mu}$ is determined by the loading conditions (which are identical to the complementary Kuhn–Tucker conditions for a truly associative structure)

$$\dot{\mu} \geqslant 0, \qquad \Phi(\bar{\boldsymbol{T}}^{\mathrm{r}}, \bar{K}) \leqslant 0, \quad \dot{\mu}\Phi(\bar{\boldsymbol{T}}^{\mathrm{r}}, \bar{K}) = 0 \tag{23}$$

Remark. In the case of viscoplasticity, $\dot{\mu}$ may be defined in the spirit of Perzyna (1963) as

$$\dot{\mu} = \frac{1}{t_*}\eta(\Phi(\bar{\boldsymbol{T}}^{\mathrm{r}}, \bar{K})) \tag{24}$$

where $\eta(\Phi)$ is the overstress function (that increases monotonically and satisfies the condition $\eta(\Phi) = 0$ if $\Phi \leqslant 0$), whereas t_* is a relaxation time. The simplest choice, is a power law of the Norton type.

The formulation of the model is complete as soon as a constitutive assumption has been introduced for the plastic spin $\bar{\boldsymbol{W}}^{\mathrm{p}} \overset{\mathrm{def}}{=} (\bar{\boldsymbol{L}}^{\mathrm{p}})^{\mathrm{skw}}$, that is associated with $\boldsymbol{F}^{\mathrm{p}}$. The simplest (and most common) choice is $\bar{\boldsymbol{W}}^{\mathrm{p}} = \dot{\mu}\bar{\boldsymbol{M}}^{\mathrm{skw}}$, which corresponds to a fully associative flow rule. Another common choice is $\bar{\boldsymbol{W}}^{\mathrm{p}} = 0$. Clearly, this results also follows from an associative flow rule in those cases when $\bar{\boldsymbol{T}}^{\mathrm{r}}$ is symmetrical. The issue of how to chose $\bar{\boldsymbol{W}}^{\mathrm{p}}$ is discussed further below.

In order to ensure that $D \geqslant 0$, it is sufficient that the following three conditions are satisfied simultaneously (indeed, to ensure that these conditions are satisfied is a key issue of the model definition):

(i) The flow rule is of the associative type (i.e. $\bar{\boldsymbol{L}}^{\mathrm{p}} = \dot{\mu}\bar{\boldsymbol{M}}$),
(ii) $\bar{\boldsymbol{\beta}}$ is symmetrical,
(iii) The identity $\bar{\boldsymbol{B}} : \dot{\bar{\boldsymbol{\beta}}} = \bar{\boldsymbol{B}} : \overset{*}{\bar{\boldsymbol{\beta}}}$ holds.

This is shown as follows: Combining (ii) with Eq. (19), we conclude that $\bar{\boldsymbol{B}}$ is symmetrical. With Eq. (21) we then obtain $\bar{\boldsymbol{B}} : \overset{*}{\bar{\boldsymbol{\beta}}} = \dot{\mu}\bar{\boldsymbol{B}} : \bar{\boldsymbol{M}}^{*}_{\mathrm{B}}$. Finally, this result together with (i) and (iii) gives

$$D = \dot{\mu}\left(\bar{\boldsymbol{T}} : \frac{\partial \Phi}{\partial \bar{\boldsymbol{T}}} + \bar{\boldsymbol{B}} : \frac{\partial \Phi}{\partial \bar{\boldsymbol{B}}} + K : \frac{\partial \Phi}{\partial K}\right) + \dot{\mu}\left(\frac{\bar{B}_{\mathrm{e}}^2}{B_\infty} + \frac{K^2}{K_\infty}\right) \geqslant 0 \tag{25}$$

In order to ensure that the spatial back-stress $\boldsymbol{b}$ is symmetrical, then, according to Eq. (8), $\bar{\boldsymbol{B}} \cdot \bar{\boldsymbol{C}}$ must be symmetrical. This condition can be satisfied only if $\bar{\boldsymbol{B}}$ is non-symmetrical in the general case. For any given $\bar{\boldsymbol{B}}^{\mathrm{sym}}$ it is possible to determine $\bar{\boldsymbol{B}}^{\mathrm{skw}}$ uniquely. However, for small elastic strains ($\bar{\boldsymbol{U}} \approx \boldsymbol{\delta}$) it is sufficient to require $\bar{\boldsymbol{B}}$ to be symmetrical $\boldsymbol{b} \approx \bar{\boldsymbol{R}} \cdot \bar{\boldsymbol{B}} \cdot \bar{\boldsymbol{R}}^{\mathrm{T}}$. To conclude, it appears to be difficult to satisfy both the condition $D \geqslant 0$ and the condition that $\boldsymbol{b}$ is symmetrical simultaneously, unless the elastic deformations are small.

Our next task is to define $\overset{*}{\bar{\boldsymbol{\beta}}}$ explicitly. To this end, we introduce $\boldsymbol{B}_{\mathrm{ref}}$ as the (co/contravariant) pull-back of $\bar{\boldsymbol{B}}$ to Ω_{ref}, and we introduce its work-conjugated variable $\boldsymbol{\beta}_{\mathrm{ref}}$ as the (contra/covariant) pull-back of $\bar{\boldsymbol{\beta}}$ to Ω_{ref} as follows:

$$\boldsymbol{B}_{\mathrm{ref}} \overset{\mathrm{def}}{=} (\boldsymbol{F}^{\mathrm{p}}_{\mathrm{ref}})^{\mathrm{T}} \cdot \bar{\boldsymbol{B}} \cdot (\boldsymbol{F}^{\mathrm{p}}_{\mathrm{ref}})^{-\mathrm{T}} \rightsquigarrow \boldsymbol{\beta}_{\mathrm{ref}} = (\boldsymbol{F}^{\mathrm{p}}_{\mathrm{ref}})^{-1} \cdot \bar{\boldsymbol{\beta}} \cdot \boldsymbol{F}^{\mathrm{p}}_{\mathrm{ref}} \tag{26}$$

A comparison with Eq. (5) shows that $\boldsymbol{B}_{\mathrm{ref}}$ is of the Mandel type in complete analogy with $\boldsymbol{T}_{\mathrm{ref}}$. Corresponding to the second term in Eq. (26), we introduce the mixed contra/covariant (Oldroyd/Rivlin) convective rate $\overset{*}{\bar{\boldsymbol{\beta}}}_{(\mathrm{OR})}$ as follows:

$$\overset{*}{\bar{\boldsymbol{\beta}}}_{(\mathrm{OR})} \overset{\mathrm{def}}{=} \boldsymbol{F}^{\mathrm{p}}_{\mathrm{ref}} \cdot \dot{\boldsymbol{\beta}}_{\mathrm{ref}} \cdot \boldsymbol{F}^{\mathrm{p}\,-1}_{\mathrm{ref}} = \dot{\bar{\boldsymbol{\beta}}} - \bar{\boldsymbol{L}}^{\mathrm{p}}_{\mathrm{ref}} \cdot \bar{\boldsymbol{\beta}} + \bar{\boldsymbol{\beta}} \cdot \bar{\boldsymbol{L}}^{\mathrm{p}}_{\mathrm{ref}} \quad \text{with} \quad \bar{\boldsymbol{L}}^{\mathrm{p}}_{\mathrm{ref}} \overset{\mathrm{def}}{=} \dot{\bar{\boldsymbol{F}}}^{\mathrm{p}}_{\mathrm{ref}} \cdot \bar{\boldsymbol{F}}^{\mathrm{p}\,-1}_{\mathrm{ref}} \tag{27}$$

which is non-symmetrical in general (even if $\bar{\boldsymbol{\beta}}$ were symmetrical). We shall, therefore, propose $\overset{*}{\bar{\boldsymbol{\beta}}}$ as follows:

$$\begin{aligned}\overset{*}{\bar{\boldsymbol{\beta}}} \overset{\mathrm{def}}{=} \frac{1}{2}\left(\overset{*}{\bar{\boldsymbol{\beta}}}_{(\mathrm{OR})} + (\overset{*}{\bar{\boldsymbol{\beta}}}_{(\mathrm{OR})})^{\mathrm{T}}\right) &= \dot{\bar{\boldsymbol{\beta}}}^{\mathrm{sym}} - \bar{\boldsymbol{D}}^{\mathrm{p}}_{\mathrm{ref}} \cdot \bar{\boldsymbol{\beta}}^{\mathrm{skw}} + \bar{\boldsymbol{\beta}}^{\mathrm{skw}} \cdot \bar{\boldsymbol{D}}^{\mathrm{p}}_{\mathrm{ref}} - \bar{\boldsymbol{W}}^{\mathrm{p}}_{\mathrm{ref}} \cdot \bar{\boldsymbol{\beta}}^{\mathrm{sym}} + \bar{\boldsymbol{\beta}}^{\mathrm{sym}} \cdot \bar{\boldsymbol{W}}^{\mathrm{p}}_{\mathrm{ref}} \\ &= \dot{\bar{\boldsymbol{\beta}}}^{\mathrm{sym}} - 2\left(\bar{\boldsymbol{D}}^{\mathrm{p}}_{\mathrm{ref}} \cdot \bar{\boldsymbol{\beta}}^{\mathrm{skw}}\right)^{\mathrm{sym}} - 2\left(\bar{\boldsymbol{W}}^{\mathrm{p}}_{\mathrm{ref}} \cdot \bar{\boldsymbol{\beta}}^{\mathrm{sym}}\right)^{\mathrm{sym}}\end{aligned} \tag{28}$$

Considering Eq. (28), we conclude that $\overset{*}{\bar{\boldsymbol{\beta}}}$ is symmetrical even when $\bar{\boldsymbol{\beta}}$ is non-symmetrical. It appears that $(\overset{*}{\bar{\boldsymbol{\beta}}}_{(\mathrm{OR})})^{\mathrm{T}} = \overset{*}{\bar{\boldsymbol{\beta}}}_{(\mathrm{RO})}$, where $\overset{*}{\bar{\boldsymbol{\beta}}}_{(\mathrm{RO})}$ is the mixed co/contravariant (Rivlin/Oldroyd) convective rate defined as follows

$$\overset{*}{\bar{\boldsymbol{\beta}}}_{(\mathrm{RO})} \overset{\mathrm{def}}{=} (\boldsymbol{F}^{\mathrm{p}}_{\mathrm{ref}})^{-\mathrm{T}} \cdot (\dot{\boldsymbol{\beta}}_{\mathrm{ref}})^{\mathrm{T}} \cdot (\boldsymbol{F}^{\mathrm{p}}_{\mathrm{ref}})^{\mathrm{T}} = \dot{\bar{\boldsymbol{\beta}}}^{\mathrm{T}} - \bar{\boldsymbol{\beta}}^{\mathrm{T}} \cdot (\bar{\boldsymbol{L}}^{\mathrm{p}}_{\mathrm{ref}})^{\mathrm{T}} + (\bar{\boldsymbol{L}}^{\mathrm{p}}_{\mathrm{ref}})^{\mathrm{T}} \cdot \bar{\boldsymbol{\beta}}^{\mathrm{T}} \tag{29}$$

Next, we shall evaluate the consequences of the formulation in Eq. (28). Combining this formulation with the rate law in Eq. (21), we obtain

$$\dot{\bar{\boldsymbol{\beta}}}^{\mathrm{sym}} = \dot{\mu}\left(\bar{\boldsymbol{M}}^{*}_{\mathrm{B}}\right)^{\mathrm{sym}} + 2\left(\bar{\boldsymbol{D}}^{\mathrm{p}}_{\mathrm{ref}} \cdot \bar{\boldsymbol{\beta}}^{\mathrm{skw}}\right)^{\mathrm{sym}} + 2\left(\bar{\boldsymbol{W}}^{\mathrm{p}}_{\mathrm{ref}} \cdot \bar{\boldsymbol{\beta}}^{\mathrm{sym}}\right)^{\mathrm{sym}} \tag{30}$$

which represents an evolution law for the symmetric part of $\bar{\boldsymbol{\beta}}$ only, and this is true for isotropic as well as anisotropic elasticity. Clearly, this fact leaves freedom in choosing a (separate) constitutive law for the skew-symmetric part of $\bar{\boldsymbol{\beta}}$.

To be specific, we shall here make the constitutive *assumption* that $\bar{\boldsymbol{\beta}}^{\mathrm{skw}} = \boldsymbol{0}$, i.e. $\bar{\boldsymbol{\beta}}$ is symmetrical, which has consequences that are investigated next. Firstly, the proper definition of $\overset{*}{\bar{\boldsymbol{\beta}}}$ is given by

$$\overset{*}{\bar{\boldsymbol{\beta}}} = \dot{\bar{\boldsymbol{\beta}}} - \bar{\boldsymbol{W}}^{\mathrm{p}}_{\mathrm{ref}} \cdot \bar{\boldsymbol{\beta}} + \bar{\boldsymbol{\beta}} \cdot \bar{\boldsymbol{W}}^{\mathrm{p}}_{\mathrm{ref}} \tag{31}$$

In this situation it appears that the rate $\overset{*}{\bar{\boldsymbol{\beta}}}$ is of the Jaumann type. Secondly, since $\bar{\boldsymbol{B}}$ and $\bar{\boldsymbol{\beta}}$ commute; they are in fact proportional, then it follows readily that

$$\bar{\boldsymbol{B}} : \left(\bar{\boldsymbol{W}}^{\mathrm{p}}_{\mathrm{ref}} \cdot \bar{\boldsymbol{\beta}} - \bar{\boldsymbol{\beta}} \cdot \bar{\boldsymbol{W}}^{\mathrm{p}}_{\mathrm{ref}}\right) = 2(\bar{\boldsymbol{B}} \cdot \bar{\boldsymbol{\beta}}) : \bar{\boldsymbol{W}}^{\mathrm{p}}_{\mathrm{ref}} = 0 \tag{32}$$

such that is concluded $\bar{\boldsymbol{B}} : \overset{*}{\bar{\boldsymbol{\beta}}} = \bar{\boldsymbol{B}} : \dot{\bar{\boldsymbol{\beta}}}$. If we, in addition, choose an associative flow rule (i), then all the condition (i)–(iii) discussed previously for ensuring that $D \geqslant 0$ are satisfied.

As to the issue of symmetry of $\boldsymbol{b}$, we recall that $\bar{\boldsymbol{B}}$ is symmetrical; however it is most unlikely that $\bar{\boldsymbol{B}}$ and $\bar{\boldsymbol{C}}$ commute. Hence, it is not possible to achieve symmetry of $\boldsymbol{b}$ using this approach.

Remark. The alternative strategy would be to choose $\bar{\boldsymbol{B}}^{\mathrm{skw}}$ in such a way that $\boldsymbol{b}$ becomes symmetrical, whereby the question arises whether it is possible to ensure that $D \geqslant 0$. However, it turns out that it is not possible to show that $\bar{\boldsymbol{B}} : \overset{*}{\bar{\boldsymbol{\beta}}} = \bar{\boldsymbol{B}} : \dot{\bar{\boldsymbol{\beta}}}$ in such a situation.

2.5. A comparison of kinematic hardening laws

In this subsection we consider special cases of the format in Eq. (31), which are obtained upon choosing Ω_{ref} appropriately. Moreover, we compare with a few suggestions in the literature.

- The PDN-format ($\bar{\boldsymbol{W}}^{\mathrm{p}}_{\mathrm{ref}} = \bar{\boldsymbol{W}}^{\mathrm{p}}$) gives

$$\overset{*}{\bar{\boldsymbol{\beta}}} = \dot{\bar{\boldsymbol{\beta}}} - \bar{\boldsymbol{W}}^{\mathrm{p}} \cdot \bar{\boldsymbol{\beta}} + \bar{\boldsymbol{\beta}} \cdot \boldsymbol{W}^{\mathrm{p}} \tag{33}$$

which bears some resemblance with the models by Tsakmakis (1996), Svendsen et al. (1998); see below.

- The PRN-format ($\bar{\boldsymbol{W}}^{\mathrm{p}}_{\mathrm{ref}} = \bar{\boldsymbol{\Omega}}^{\mathrm{p}}_{\mathrm{ref}} = \bar{\boldsymbol{\Omega}}^{\mathrm{p}} \overset{\mathrm{def}}{=} \dot{\boldsymbol{R}}^{\mathrm{p}} \cdot (\boldsymbol{R}^{\mathrm{p}})^{\mathrm{T}}$ and $\bar{\boldsymbol{D}}^{\mathrm{p}}_{\mathrm{ref}} = 0$) gives

$$\overset{*}{\bar{\boldsymbol{\beta}}} = \dot{\bar{\boldsymbol{\beta}}} - \bar{\boldsymbol{\Omega}}^{\mathrm{p}} \cdot \bar{\boldsymbol{\beta}} + \bar{\boldsymbol{\beta}} \cdot \bar{\boldsymbol{\Omega}}^{\mathrm{p}} \tag{34}$$

which was defined by Münz et al. (1999). This format is identical to the PDN format when $\bar{\boldsymbol{W}}^{\mathrm{p}} = \bar{\boldsymbol{\Omega}}^{\mathrm{p}}$.

- The UR-format ($\bar{\boldsymbol{W}}^{\mathrm{p}}_{\mathrm{ref}} = 0$) gives $\overset{*}{\bar{\boldsymbol{\beta}}} = \dot{\bar{\boldsymbol{\beta}}}$. This format represents a direct generalization to large deformations of the small strain model by Chaboche et al. (1979). It has been investigated by, e.g. Eterovic and Bathe (1990). We note that the UR-format is identical to the PDN-format when $\bar{\boldsymbol{W}}^{\mathrm{p}} = 0$ (which is the most basic assumption adopted in the constitutive rate law for $\boldsymbol{F}^{\mathrm{p}}$). The corresponding model is known to perform poorly in the case of simple shear, in which case the shear stress shows the pathological oscillatory behavior that is typical for Jaumann-type hypoelasticity-based formulations, cf. Svendsen et al. (1998), Münz et al. (1999).

A model that is related to the one suggested by Schieck and Stumpf (1995) is defined by $\boldsymbol{F}^{\mathrm{p}}_{\mathrm{ref}} = \boldsymbol{R}^{\mathrm{ep}} \overset{\mathrm{def}}{=} \bar{\boldsymbol{R}} \cdot \boldsymbol{R}^{\mathrm{p}}$, which gives $\bar{\boldsymbol{W}}^{\mathrm{p}} = \boldsymbol{\Omega}^{\mathrm{ep}} = \dot{\boldsymbol{R}}^{\mathrm{ep}} \cdot (\boldsymbol{R}^{\mathrm{ep}})^{\mathrm{T}}$. The corresponding convective rate, denoted the SS-rate by Schieck and Stumpf (1995), is given as

$$\overset{*}{\bar{\boldsymbol{\beta}}} = \dot{\bar{\boldsymbol{\beta}}} - \boldsymbol{\Omega}^{\mathrm{ep}} \cdot \bar{\boldsymbol{\beta}} + \bar{\boldsymbol{\beta}} \cdot \boldsymbol{\Omega}^{\mathrm{ep}} \tag{35}$$

Finally, we mention a model proposed by Svendsen et al. (1998), which can be retrieved as follows: Let $\bar{\boldsymbol{\beta}}$ transform as a second PK-stress tensor, such that $\boldsymbol{\beta}_{\mathrm{ref}}$ is obtained from

$$\boldsymbol{\beta}_{\mathrm{ref}} = (\boldsymbol{F}^{\mathrm{p}})^{-1} \cdot \bar{\boldsymbol{\beta}} \cdot (\boldsymbol{F}^{\mathrm{p}})^{-\mathrm{T}} \tag{36}$$

Corresponding to Eq. (36), it is possible to introduce the contra/contravariant convective rate (of the Oldroyd type) as follows:

$$\overset{*}{\bar{\boldsymbol{\beta}}} = \overset{*}{\bar{\boldsymbol{\beta}}}_{(\mathrm{OO})} \overset{\mathrm{def}}{=} \boldsymbol{F}^{\mathrm{p}} \cdot \dot{\boldsymbol{\beta}}_{\mathrm{ref}} \cdot (\boldsymbol{F}^{\mathrm{p}})^{\mathrm{T}} = \dot{\bar{\boldsymbol{\beta}}} - \bar{\boldsymbol{L}}^{\mathrm{p}} \cdot \bar{\boldsymbol{\beta}} - \bar{\boldsymbol{\beta}} \cdot (\bar{\boldsymbol{L}}^{\mathrm{p}})^{\mathrm{T}} \tag{37}$$

2.6. Auxiliary kinematic considerations

We note that $\bar{\boldsymbol{\Omega}}^{\mathrm{p}}$ can be computed from $\bar{\boldsymbol{D}}^{\mathrm{p}}$ and $\bar{\boldsymbol{W}}^{\mathrm{p}}$ via pure kinematics. In order to derive the pertinent relation, we combine the definition $\bar{\boldsymbol{L}}^{\mathrm{p}} = \dot{\boldsymbol{F}}^{\mathrm{p}} \cdot (\boldsymbol{F}^{\mathrm{p}})^{-1}$ with the decomposition $\boldsymbol{F}^{\mathrm{p}} = \boldsymbol{R}^{\mathrm{p}} \cdot \boldsymbol{U}^{\mathrm{p}}$ to obtain the relations

$$\bar{\boldsymbol{D}}^{\mathrm{p}} = \tfrac{1}{2}\boldsymbol{R}^{\mathrm{p}} \cdot (\dot{\boldsymbol{U}}^{\mathrm{p}} \cdot (\boldsymbol{U}^{\mathrm{p}})^{-1})^{\mathrm{sym}} \cdot (\boldsymbol{R}^{\mathrm{p}})^{\mathrm{T}} \tag{38}$$

$$\bar{\boldsymbol{W}}^{\mathrm{p}} = \bar{\boldsymbol{\Omega}}^{\mathrm{p}} + \tfrac{1}{2}\boldsymbol{R}^{\mathrm{p}} \cdot (\dot{\boldsymbol{U}}^{\mathrm{p}} \cdot (\boldsymbol{U}^{\mathrm{p}})^{-1})^{\mathrm{skw}} \cdot (\boldsymbol{R}^{\mathrm{p}})^{\mathrm{T}} \tag{39}$$

Hence, for given $\bar{\boldsymbol{D}}^{\mathrm{p}}$, it is possible to solve for $\dot{\boldsymbol{U}}^{\mathrm{p}}$ from Eq. (38) as follows:

$$\dot{\boldsymbol{U}}^{\mathrm{p}} = 2\mathscr{A}^{-1} : ((\boldsymbol{R}^{\mathrm{p}})^{\mathrm{T}} \cdot \bar{\boldsymbol{D}}^{\mathrm{p}} \cdot \boldsymbol{R}^{\mathrm{p}}) \tag{40}$$

where $\mathscr{A}$ is the fourth order tensor [2]

$$\mathscr{A} = \tfrac{1}{2}(\boldsymbol{\delta}\,\overline{\otimes}\,(\boldsymbol{U}^{\mathrm{p}})^{-1} + (\boldsymbol{U}^{\mathrm{p}})^{-1}\,\overline{\otimes}\,\boldsymbol{\delta} + \boldsymbol{\delta}\,\underline{\otimes}\,(\boldsymbol{U}^{\mathrm{p}})^{-1} + (\boldsymbol{U}^{\mathrm{p}})^{-1}\,\underline{\otimes}\,\boldsymbol{\delta}) \tag{41}$$

that possesses major as well as minor symmetry, i.e. $\mathscr{A}_{ijkl} = \mathscr{A}_{klij} = \mathscr{A}_{jikl} = \mathscr{A}_{ijlk}$. Inserting $\dot{\boldsymbol{U}}^{\mathrm{p}}$ from Eq. (40) into Eq. (39), we obtain

$$\bar{\boldsymbol{\Omega}}^{\mathrm{p}} = \bar{\boldsymbol{W}}^{\mathrm{p}} - \bar{\boldsymbol{W}}^{\mathrm{p}}_{\mathrm{D}}(\bar{\boldsymbol{D}}^{\mathrm{p}}; \boldsymbol{R}^{\mathrm{p}}, \boldsymbol{U}^{\mathrm{p}}) \tag{42}$$

where it is noted that $\bar{\boldsymbol{W}}^{\mathrm{p}}_{\mathrm{D}}$ is a first order homogeneous function in its first argument.

The following special cases are of interest:

- No plastic spin ($\bar{\boldsymbol{W}}^{\mathrm{p}} = 0$) infers that $\bar{\boldsymbol{\Omega}}^{\mathrm{p}} = -\bar{\boldsymbol{W}}^{\mathrm{p}}_{\mathrm{D}}(\bar{\boldsymbol{D}}^{\mathrm{p}}; \boldsymbol{R}^{\mathrm{p}}, \boldsymbol{U}^{\mathrm{p}})$ for given $\bar{\boldsymbol{D}}^{\mathrm{p}}$.
- No plastic rotation ($\boldsymbol{R}^{\mathrm{p}} = \boldsymbol{\delta}$) infers that $\bar{\boldsymbol{\Omega}}^{\mathrm{p}} = 0$ and, hence, $\bar{\boldsymbol{W}}^{\mathrm{p}} = \bar{\boldsymbol{W}}^{\mathrm{p}}_{\mathrm{D}}(\bar{\boldsymbol{D}}^{\mathrm{p}}; \boldsymbol{\delta}, \boldsymbol{U}^{\mathrm{p}})$ for given $\bar{\boldsymbol{D}}^{\mathrm{p}}$.
- No elastic rotation ($\boldsymbol{R}^{\mathrm{p}} = \boldsymbol{R}$) infers that $\bar{\boldsymbol{\Omega}}^{\mathrm{p}} = \boldsymbol{\Omega} = \dot{\boldsymbol{R}} \cdot \boldsymbol{R}^{\mathrm{T}}$ and, hence, $\bar{\boldsymbol{W}}^{\mathrm{p}} = \boldsymbol{\Omega} + \bar{\boldsymbol{W}}^{\mathrm{p}}_{\mathrm{D}}(\bar{\boldsymbol{D}}^{\mathrm{p}}; \boldsymbol{R}, \boldsymbol{U}^{\mathrm{p}})$ for given $\bar{\boldsymbol{D}}^{\mathrm{p}}$.

3. Incremental format of constitutive relations

3.1. "Exact" integration algorithm

In quite standard fashion we apply the (exponential) Backward Euler rule, see Weber and Anand (1990), to integrate the flow rule in (20): [3]

$$\boldsymbol{F}^{\mathrm{p}} = \bar{\boldsymbol{A}} \cdot {}^{n}\boldsymbol{F}^{\mathrm{p}} \quad \text{with} \quad \bar{\boldsymbol{A}} = \exp(\Delta\mu\bar{\boldsymbol{M}}^{\mathrm{sym}} + \Delta t\bar{\boldsymbol{W}}^{\mathrm{p}}) \tag{43}$$

From $\bar{\boldsymbol{F}} = \boldsymbol{F} \cdot (\boldsymbol{F}^{\mathrm{p}})^{-1}$ we then obtain

$$\bar{\boldsymbol{F}} = \bar{\boldsymbol{F}}^{\mathrm{trial}} \cdot \bar{\boldsymbol{A}}^{-1} \quad \text{with} \quad \bar{\boldsymbol{F}}^{\mathrm{trial}} \stackrel{\mathrm{def}}{=} \boldsymbol{F} \cdot ({}^{n}\boldsymbol{F}^{\mathrm{p}})^{-1} \tag{44}$$

and we can compute $\bar{\boldsymbol{C}}$ from the "trial" deformation $\bar{\boldsymbol{C}}^{\mathrm{trial}}$

$$\bar{\boldsymbol{C}} = \bar{\boldsymbol{F}}^{\mathrm{T}} \cdot \bar{\boldsymbol{F}} = \bar{\boldsymbol{A}}^{-\mathrm{T}} \cdot \bar{\boldsymbol{C}}^{\mathrm{trial}} \cdot \bar{\boldsymbol{A}}^{-1} \quad \text{with} \quad \bar{\boldsymbol{C}}^{\mathrm{trial}} \stackrel{\mathrm{def}}{=} \boldsymbol{C}({}^{n}\boldsymbol{F}^{\mathrm{p}})^{-\mathrm{T}} \cdot {}^{n}\boldsymbol{F}^{\mathrm{p}} \tag{45}$$

Next, we consider the kinematic hardening and rewrite Eq. (29) as follows:

[2] For second order tensors $\boldsymbol{A}$ and $\boldsymbol{B}$, we define $(\boldsymbol{A}\,\overline{\otimes}\,\boldsymbol{B})_{ijkl} = A_{ik}B_{jl}$, $(\boldsymbol{A}\,\underline{\otimes}\,\boldsymbol{B})_{ijkl} = A_{il}B_{jk}$.

[3] Values at time t_n are denoted by left superscript n; however, to abbreviate notation the superscript $n+1$ (denoting updated values at time t_{n+1}) is omitted.

$$\dot{\boldsymbol{\beta}}_{\rm ref} = (\boldsymbol{F}^{\rm p}_{\rm ref})^{-1} \cdot \overset{*}{\bar{\boldsymbol{\beta}}}_{(\rm OR)} \cdot \boldsymbol{F}^{\rm p}_{\rm ref} \tag{46}$$

Upon applying the Backward Euler rule to Eq. (46), we obtain

$$\boldsymbol{\beta}_{\rm ref} = {}^{n}\boldsymbol{\beta}_{\rm ref} + (\boldsymbol{F}^{\rm p}_{\rm ref})^{-1} \cdot \Delta t\, \overset{*}{\bar{\boldsymbol{\beta}}}_{(\rm OR)} \cdot \boldsymbol{F}^{\rm p}_{\rm ref} \tag{47}$$

Now, introducing the operator $\bar{\boldsymbol{A}}_{\rm ref}$, in analogy with Eq. (43) via the decomposition $\boldsymbol{F}^{\rm p}_{\rm ref} = \bar{\boldsymbol{A}}_{\rm ref} \cdot {}^{n}\boldsymbol{F}^{\rm p}_{\rm ref}$ and combining with Eq. (26), we obtain from Eq. (47)

$$\bar{\boldsymbol{\beta}} = \boldsymbol{F}^{\rm p}_{\rm ref} \cdot {}^{n}\boldsymbol{\beta}_{\rm ref} \cdot (\boldsymbol{F}^{\rm p}_{\rm ref})^{-1} + \Delta t \overset{*}{\bar{\boldsymbol{\beta}}}_{(\rm OR)} = \bar{\boldsymbol{A}}_{\rm ref} \cdot {}^{n}\bar{\boldsymbol{\beta}} \cdot (\bar{\boldsymbol{A}}_{\rm ref})^{-1} + \Delta t \overset{*}{\bar{\boldsymbol{\beta}}}_{(\rm OR)} \tag{48}$$

Taking the symmetric part of Eq. (48), while using the hardening rule in Eq. (21), we finally obtain

$$\bar{\boldsymbol{\beta}} = \bar{\bar{\boldsymbol{\beta}}} + \Delta\mu(\bar{\boldsymbol{M}}^{*}_{\rm B})^{\rm sym} \quad \text{with} \quad \bar{\bar{\boldsymbol{\beta}}} \overset{\rm def}{=} (\bar{\boldsymbol{A}}_{\rm ref} \cdot {}^{n}\bar{\boldsymbol{\beta}} \cdot (\bar{\boldsymbol{A}}_{\rm ref})^{-1})^{\rm sym} \tag{49}$$

Finally, we integrate Eq. (22) to obtain

$$\kappa = {}^{n}\kappa + \Delta\mu M^{*}_{K} \tag{50}$$

We may now summarize the constitutive relations as follows:

$$\begin{aligned}
&\boldsymbol{Y}_{\bar{\rm C}} = \bar{\boldsymbol{C}} - \bar{\boldsymbol{A}}^{-\rm T} \cdot \bar{\boldsymbol{C}}^{\rm trial} \cdot \bar{\boldsymbol{A}}^{-1} = \boldsymbol{0}\\
&\boldsymbol{Y}_{\bar{\rm A}^{-1}} = \bar{\boldsymbol{A}}^{-1} - \exp(-\Delta\mu\bar{\boldsymbol{M}}^{\rm sym} - \Delta t\bar{\boldsymbol{W}}^{\rm p}) = \boldsymbol{0}\\
&\boldsymbol{Y}_{\bar{\beta}} = \bar{\boldsymbol{\beta}} - \bar{\bar{\boldsymbol{\beta}}} - \Delta\mu(\bar{\boldsymbol{M}}^{*}_{\rm B})^{\rm sym} = \boldsymbol{0}\\
&Y_{\kappa} = \kappa - {}^{n}\kappa - \Delta\mu M^{*}_{K} = 0\\
&\Delta\mu \geqslant 0, \quad \Phi \leqslant 0, \quad \Delta\mu\Phi = 0
\end{aligned} \tag{51}$$

where $\bar{\bar{\boldsymbol{\beta}}}$ is defined as

$$\bar{\bar{\boldsymbol{\beta}}} = \begin{cases} \boldsymbol{R}^{\rm p} \cdot ({}^{n}\boldsymbol{R}^{\rm p})^{\rm T} \cdot {}^{n}\bar{\boldsymbol{\beta}} \cdot {}^{n}\boldsymbol{R}^{\rm p} \cdot (\boldsymbol{R}^{\rm p})^{\rm T} & \text{PRN-model} \\ \bar{\boldsymbol{A}} \cdot {}^{\rm b}\bar{\boldsymbol{\beta}} \cdot \bar{\boldsymbol{A}}^{\rm T} & \text{PDNSv-model} \end{cases} \tag{52}$$

The PDNSv-model is defined by Eqs. (36) and (37), cf. Svenden et al. (1998). It is denoted that $\bar{\boldsymbol{A}}$ is a function of $\Delta\mu, \bar{\boldsymbol{M}}$ and $\Delta t\bar{\boldsymbol{W}}^{\rm p}$. Both $\bar{\boldsymbol{M}}$ and $\bar{\boldsymbol{M}}^{*}_{\rm B}$ are functions of $\bar{\boldsymbol{C}}$ and $\bar{\boldsymbol{\beta}}$ via the relations $\bar{\boldsymbol{T}}(\bar{\boldsymbol{C}})$ and $\bar{\boldsymbol{B}}(\bar{\boldsymbol{\beta}})$, whereas M^{*}_{K} is a function of κ via the relation $K(\kappa)$. Moreover, the flow function Φ is a function of $\bar{\boldsymbol{C}}$, $\bar{\boldsymbol{\beta}}$ and κ via the functional relations $\bar{\boldsymbol{T}}(\bar{\boldsymbol{C}})$, $\bar{\boldsymbol{B}}(\bar{\boldsymbol{\beta}})$ and $\bar{K}(\bar{\kappa})$, which were given in Eqs. (16) and (19), respectively. It turns out that these relations are completely analogous to those pertinent to geometrically linear theory.

In the case of plastic loading, we may abbreviate Eq. (51) (on matrix form) as follows: $\underline{\boldsymbol{Y}}(\underline{\boldsymbol{X}}) = \underline{0}$, where $\underline{\boldsymbol{X}}$ contains the components of all unknowns, whereas $\underline{\boldsymbol{Y}}$ contains the corresponding residuals, i.e.

$$\begin{aligned}
&\underline{\boldsymbol{X}} = [\bar{\boldsymbol{C}},\ \bar{\boldsymbol{A}}^{-1},\ \bar{\boldsymbol{\beta}}, \kappa,\ \Delta\mu]^{\rm T}\\
&\underline{\boldsymbol{Y}} = [\boldsymbol{Y}_{\bar{\rm C}},\ \boldsymbol{Y}_{\bar{\rm A}^{-1}},\ \boldsymbol{Y}_{\bar{\beta}},\ Y_{\kappa},\ Y_{\Delta\mu}]^{\rm T} \quad \text{with} \quad Y_{\Delta\mu} = \Phi
\end{aligned} \tag{53}$$

It remains to define $\Delta t\bar{\boldsymbol{W}}^{\rm p}$. The "main" situation is that the flow rule is associative, in which case $\Delta t\bar{\boldsymbol{W}}^{\rm p} = \Delta\mu\bar{\boldsymbol{M}}^{\rm skw}$. Other special cases are:

- No plastic spin ($\bar{\boldsymbol{W}}^{\rm p} = 0$) infers that $\Delta t\bar{\boldsymbol{W}}^{\rm p} = 0$. (This is also obtained in the case of an associative flow rule when $\bar{\boldsymbol{M}}$ is symmetrical, e.g. for isotropic elasticity.)
- No plastic rotation ($\boldsymbol{R}^{\rm p} = \boldsymbol{\delta}$), infers that $\Delta t\bar{\boldsymbol{W}}^{\rm p} = \Delta\mu\bar{\boldsymbol{W}}^{\rm p}_{\rm D}(\bar{\boldsymbol{M}}^{\rm sym}; \boldsymbol{\delta}, \boldsymbol{U}^{\rm p})$
- No elastic rotation ($\boldsymbol{R}^{\rm p} = \boldsymbol{R}$) infers that

$$\Delta t \bar{\boldsymbol{W}}^{\mathrm{p}} = \ln(\boldsymbol{R}\cdot{}^{n}\boldsymbol{R}^{\mathrm{T}}) + \Delta\mu\bar{\boldsymbol{W}}^{\mathrm{p}}_{\mathrm{D}}(\bar{\boldsymbol{M}}^{\mathrm{sym}};\boldsymbol{R},\boldsymbol{U}^{\mathrm{p}})$$

In order to obtain the last result (for $\boldsymbol{R}^{\mathrm{p}} = \boldsymbol{R}$) we integrated the relation $\Omega = \dot{\boldsymbol{R}}\cdot\boldsymbol{R}^{\mathrm{T}}$ using the exponential Backward Euler rule, i.e.

$$\exp(\Delta t\Omega) = \boldsymbol{R}\cdot({}^{n}\boldsymbol{R})^{\mathrm{T}} \tag{54}$$

which is incrementally objective.

3.2. "Linearized" integration algorithm

When $\bar{\boldsymbol{C}}$, $\bar{\boldsymbol{C}}^{\mathrm{trial}}$ and $\bar{\boldsymbol{A}}$ (and $\bar{\boldsymbol{M}}$) commute, it is possible to use the summation rules for logarithms to obtain from Eq. (45) the commonly used decomposition

$$\ln(\bar{\boldsymbol{C}}) = \ln(\boldsymbol{C}^{\mathrm{trial}}) - 2\Delta\mu\bar{\boldsymbol{M}}^{\mathrm{sym}} \tag{55}$$

This is, indeed, the case for isotropic elasticity and purely isotropic hardening. However, when non-coaxiality is present Eq. (55) introduces additional approximation (truncation error). For example, the spin $\bar{\boldsymbol{W}}^{\mathrm{p}}$ is completely lost. Nevertheless, it may be tempting to use this approximation, at least in combination with the replacement of $\bar{\bar{\boldsymbol{\beta}}}$ in Eq. (52) with ${}^{n}\bar{\bar{\boldsymbol{\beta}}}$ defined as

$${}^{n}\bar{\bar{\boldsymbol{\beta}}} = \begin{cases} {}^{n}\boldsymbol{R}^{\mathrm{p}}\cdot({}^{n-1}\boldsymbol{R}^{\mathrm{p}})^{\mathrm{T}}\cdot{}^{n}\bar{\boldsymbol{\beta}}\cdot{}^{n-1}\boldsymbol{R}^{\mathrm{p}}\cdot({}^{n}\boldsymbol{R}^{\mathrm{p}})^{\mathrm{T}} & \text{PRN-model} \\ {}^{n}\bar{\boldsymbol{A}}\cdot{}^{n}\bar{\boldsymbol{\beta}}\cdot{}^{n}\bar{\boldsymbol{A}}^{\mathrm{T}} & \text{PDNSv-model} \end{cases} \tag{56}$$

The resulting algorithm represents mixed implicit/explicit integration of the pertinent evolution equations

Remark. It is noted that the formulation in Eq. (56) does *not* follow from simply setting $\boldsymbol{R}^{\mathrm{p}} = {}^{n}\boldsymbol{R}^{\mathrm{p}}$ in Eq. (52), which would infer that $\bar{\bar{\boldsymbol{\beta}}} = {}^{n}\bar{\boldsymbol{\beta}}$, pertinent to the UR-format.

Summarizing the linearized algorithm (subsequently abbreviated $\mathrm{BE_{lin}}$), we note that the formulation will be identical to that of small strains, which has since long been utilized for isotropic hardening. In particular, in the case of linear hardening, a linear relation in $\Delta\mu$ is obtained; hence, no iterations are necessary to solve the "local problem" for given $\bar{\boldsymbol{C}}^{\mathrm{trial}}$.

3.3. Local problem and ATS-tensor

The ATS tensor $\mathscr{L}^{a}_{2}$ on Ω_0 is defined from the generic relation

$$\mathscr{L}^{a}_{2} = 2\frac{\mathrm{d}\boldsymbol{S}_2}{\mathrm{d}\boldsymbol{C}} \tag{57}$$

which is derived in the following fashion: Differentiating the first part of basic relation (2), we obtain

$$\frac{\mathrm{d}\boldsymbol{S}_2}{\mathrm{d}\boldsymbol{C}} = \frac{1}{2}\left((\boldsymbol{F}^{\mathrm{p}})^{-1}\overline{\otimes}(\boldsymbol{F}^{\mathrm{p}})^{-1}\right) : \bar{\mathscr{L}}^{\mathrm{e}}_{2} : \frac{\mathrm{d}\bar{\boldsymbol{C}}}{\mathrm{d}\boldsymbol{C}} + \left[({}^{n}\boldsymbol{F}^{\mathrm{p}})^{-1}\overline{\otimes}\left((\boldsymbol{F}^{\mathrm{p}})^{-1}\cdot\bar{\boldsymbol{S}}_2\right) + \left((\boldsymbol{F}^{\mathrm{p}})^{-1}\cdot\bar{\boldsymbol{S}}_2\right)\underline{\otimes}({}^{n}\boldsymbol{F}^{\mathrm{p}})^{-1}\right] : \frac{\mathrm{d}\bar{\boldsymbol{A}}^{-1}}{\mathrm{d}\boldsymbol{C}} \tag{58}$$

where we used the relation (43) and introduced the elastic tangent stiffness $\bar{\mathscr{L}}^{\mathrm{e}}_{2} = 2\mathrm{d}\bar{\boldsymbol{S}}_2/\mathrm{d}\bar{\boldsymbol{C}}$. The tensors $\mathrm{d}\bar{\boldsymbol{A}}^{-1}/\mathrm{d}\boldsymbol{C}$ and $\mathrm{d}\bar{\boldsymbol{C}}/\mathrm{d}\boldsymbol{C}$ can then be computed via the Jacobian $\underline{\boldsymbol{J}}$ of the *local* problem (53):

$$\underline{\boldsymbol{Y}}(\underline{\boldsymbol{X}}(\bar{\boldsymbol{C}}^{\mathrm{trial}});\bar{\boldsymbol{C}}^{\mathrm{trial}}) = \underline{\boldsymbol{0}} \quad \forall\bar{\boldsymbol{C}}^{\mathrm{trial}} \rightsquigarrow \frac{\mathrm{d}\underline{\boldsymbol{X}}}{\mathrm{d}\bar{\boldsymbol{C}}^{\mathrm{trial}}} = -\underline{\boldsymbol{J}}^{-1}\frac{\partial\underline{\boldsymbol{Y}}}{\partial\bar{\boldsymbol{C}}^{\mathrm{trial}}} \tag{59}$$

4. Numerical results

4.1. Preliminaries

At the numerical investigation of simple shear and unconstrained shear the following values of the material parameters were used: $E = 210 \times 10^3$ MPa, $\nu = 0.3$, $\sigma_y = 500$ MPa, $H = 1.5 \times 10^3$ MPa. Only linear hardening, defined by $K_\infty = B_\infty = \infty$, was considered, since the nonlinear hardening feature has little significance for the present purpose of analysis. The angle θ defines the "direction of elastic anisotropy", as shown in Fig. 2a, whereas the simple shear kinematics is given in Fig. 2b.

4.2. Stress–strain response relation for simple shear – model performance

In Figs. 3 and 4 we compare the model performance in simple shear of the PRN-model (Fig. 3) and the PDNSv-model (Fig. 4) for both isotropic and kinematic hardening. Isotropic elasticity and associative flow ($\bar{\boldsymbol{W}}^{\mathrm{p}} = \boldsymbol{0}$) are assumed. The in-plane stress ans back-stress components in the spatial format are plotted

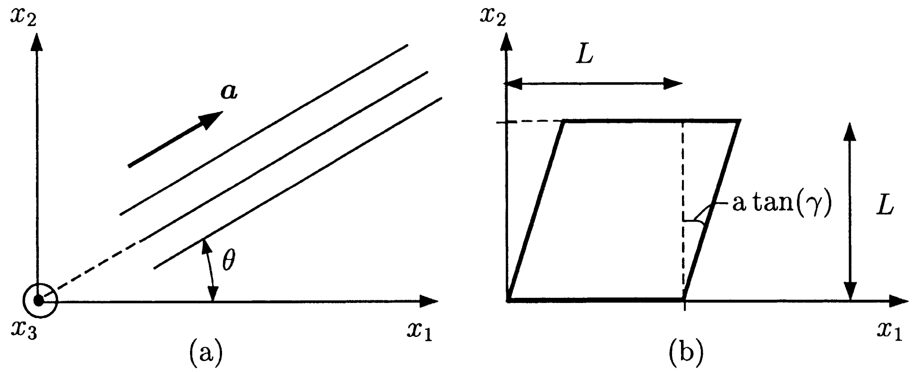

Fig. 2. (a) Elastic anisotropy direction defined by θ, (b) kinematics for simple shear and the relation $\mathrm{d}\bar{\boldsymbol{C}}^{\mathrm{trial}}/\mathrm{d}\boldsymbol{C} = ({}^n\boldsymbol{F}^{\mathrm{p}})^{-\mathrm{T}} \bar{\otimes} ({}^n\mathbf{F}^{\mathrm{p}})^{-\mathrm{T}}$, which is obtained from Eq. (45).

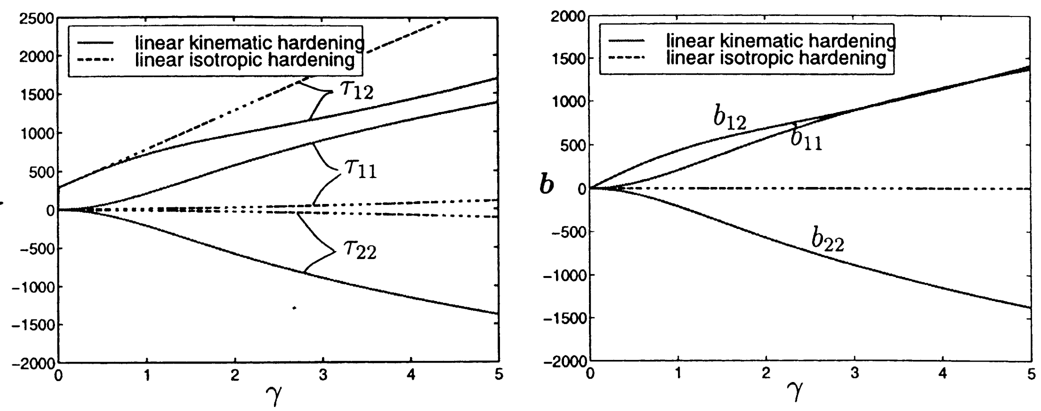

Fig. 3. In-plane stress $\boldsymbol{\tau}$ and back-stress $\boldsymbol{b}$ components versus shear deformation γ for the PRN-model with isotropic elasticity, linear kinematic hardening ($r = 0$) and linear isotropic hardening ($r = 1$).

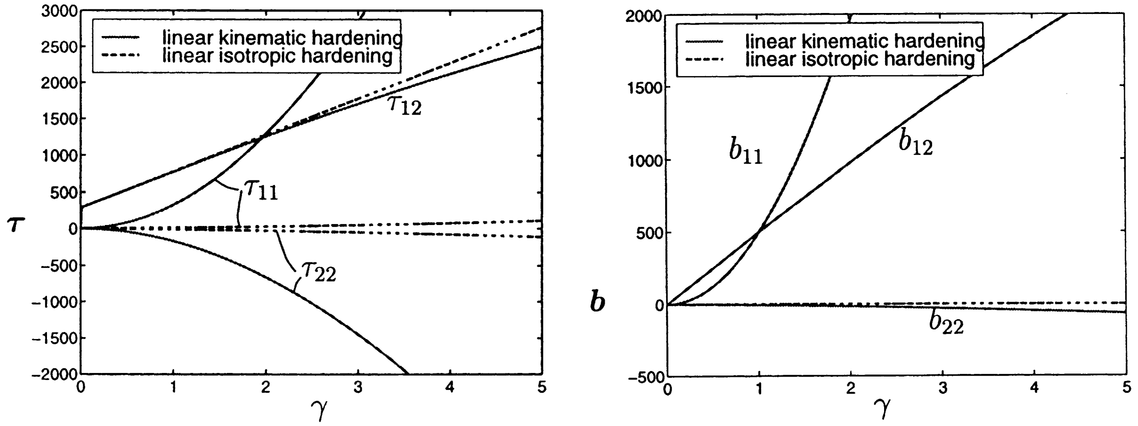

Fig. 4. In-plane stress τ and back-stress b components versus shear deformation γ for the PDNSv-model with isotropic elasticity, linear kinematic hardening ($r = 0$) and linear isotropic hardening ($r = 1$).

against the shear deformation γ. In the case of kinematic hardening, we conclude: For the PRN-model the normal stresses are "anti-symmetrical" in the sense that $\tau_{11} = -\tau_{22}$ and $b_{11} = -b_{22}$, whereas this is not so for the PDNSv-model. However, the shear stress satisfies the assumption of linearity better for the PDNSv-model. The next series of computations concerned the influence of plastic rotation, whereby the different strategies for imposing $\boldsymbol{R}^{\mathrm{p}}$ are defined by the appropriate choice of $\Delta t\bar{\boldsymbol{W}}^{\mathrm{p}}$. Three strategies were considered: (i) Associative flow, (ii) no plastic rotation ($\boldsymbol{R}^{\mathrm{p}} = \boldsymbol{\delta}$), (iii) no elastic rotation ($\boldsymbol{R}^{\mathrm{p}} = \boldsymbol{R}$). The corresponding choice of $\Delta t\bar{\boldsymbol{W}}^{\mathrm{p}}$ was defined in Section 3.1. Firstly, the three strategies were checked in conjunction with isotropic elasticity, and it was readily confirmed (not shown here) that the amount of plastic rotation does not have any effect on the results. (This fact, which is expected due to the isotropic elasticity, was pointed out by Simo (1988).) Secondly, the effect of rotation was found to be considerable in the presence of anisotropy ($\theta = 90°$) which is shown in Fig. 5 for the PRN-model.

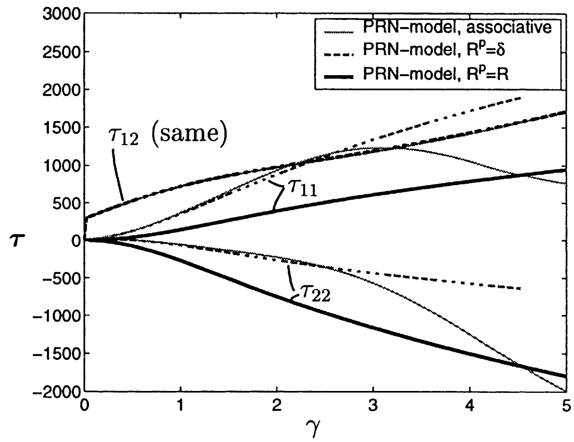

Fig. 5. In-plane stress τ components versus deformation γ for the PRN-model with transversely isotropic elasticity ($\theta = 90°$) and kinematic hardening. Influence of plastic rotation.

Since the shear modulus was isotropic ($G_{\|} = G$), only the normal stresses were affected by the rotation. If of interest to assess the magnitude of non-symmetry of $\boldsymbol{b}$, which may be measured as $|\boldsymbol{b}^{\text{skw}}|/|\boldsymbol{b}|$. Indeed, since the elastic deformations were small, this ratio was found to be very small.

4.3. Stress–strain response for simple shear – influence of "linearization" in the integration algorithm

A series of computations were carried out to demonstrate the (possible) effect of "linearization" of the incremental algorithm for the simple shear problem. Figs. 6 and 7 show results for the PRN-model with two different resolutions of the integration algorithm (uniform timesteps), whereas Figs. 8 and 9 show the corresponding results for the PDNSv-model. The significance of "linearization" is noticeable for both

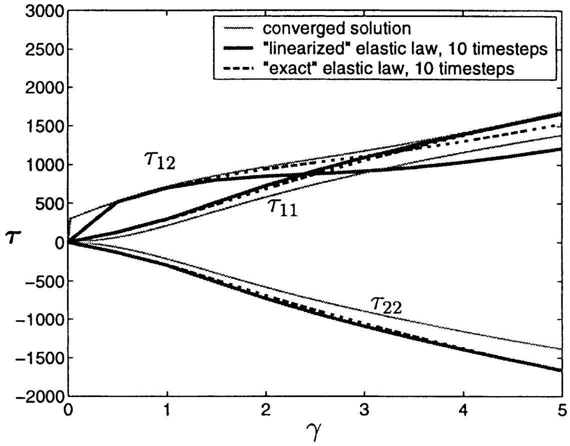

Fig. 6. In-plane stress $\boldsymbol{\tau}$ components versus shear deformation γ for the PRN-model with isotropic elasticity, associative flow rule and kinematic hardening. Influence of algorithm "linearization".

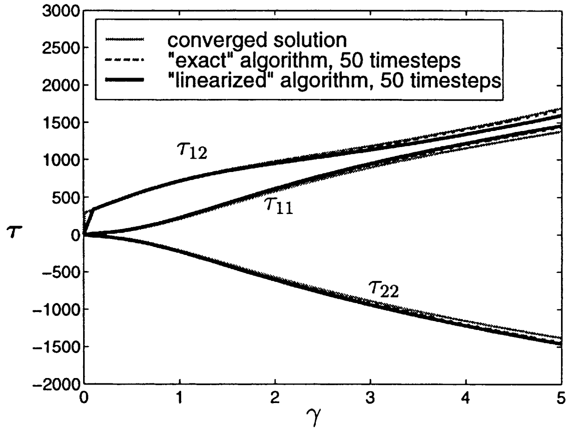

Fig. 7. In-plane stress $\boldsymbol{\tau}$ components versus shear deformation γ for the PRN-model with isotropic elasticity, associative flow rule and kinematic hardening. Influence of algorithm "linearization".

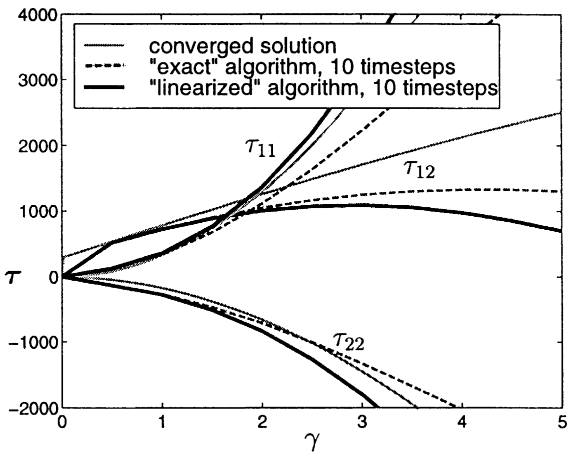

Fig. 8. In-plane stress τ components versus shear deformation γ for the PDNSv-model with isotropic elasticity, associative flow rule and kinematic hardening. Influence of algorithm "linearization".

models. However, it is also confirmed that even the linearized algorithm ensures convergence to the true answer when the time increments become small; i.e. this method is at least consistent (of first order). It is also noticed that the convergence is slower for the PDNSv-model.

The additional truncation error due to the non-coaxiality when the logarithm product formula is used is evaluated a posteriori. One possibility is to use the "exact" format and to compare the "linearized" elastic strains $\bar{\boldsymbol{C}}_{(\text{linear})}$ defined as

$$\bar{\boldsymbol{C}}_{(\text{linear})} = \exp(\ln(\bar{\boldsymbol{C}}^{\text{trial}}) - 2\Delta\mu\bar{\boldsymbol{M}}^{\text{sym}}) \tag{60}$$

with the "exact" elastic strain $\bar{\boldsymbol{C}}_{(\text{exact})}$. The error e is defined as

$$e = \frac{|\bar{\boldsymbol{C}}_{(\text{exact})} - \bar{\boldsymbol{C}}_{(\text{linear})}|}{|\bar{\boldsymbol{C}}_{(\text{exact})}|} \tag{61}$$

and is shown in Fig. 10 for the PRN-model (for the set of data used in Figs. 6 and 7). Furthermore, Fig. 11 shows results for the PRN-model in the presence of transversely isotropic elasticity, which leads to even larger truncation errors when the linearized algorithm is used.

The last series of computations show the effect of linearization when the unconstrained shear problem [4] is analyzed using finite elements (16 triangular elements with piecewise linear displacements). Even in this case the influence of discretization errors in time become pronounced, cf. Fig. 12.

5. Concluding remarks

Certain consequences of elastic and plastic anisotropy for a particular class of hyperelastic–plastic models with kinematic hardening were investigated in this paper. In particular, we have considered the

[4] Referring to Fig. 2(b), the displacement field is represented by the components $u_i(X_1, X_2)$, $X_i \in (0, L)$. The unconstrained shear problem is defined by the boundary conditions $u_i(X_1, 0) = 0, u_1(X_1, L) = \bar{u}_1(t)$ (prescribed) and $u_2(X_1, L) = 0$.

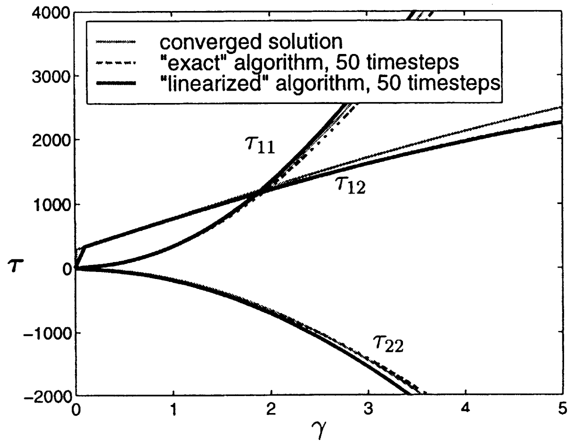

Fig. 9. In-plane stress τ components versus shear deformation γ for the PDNSv-model with isotropic elasticity, associative flow rule and kinematic hardening. Influence of algorithm "linearization".

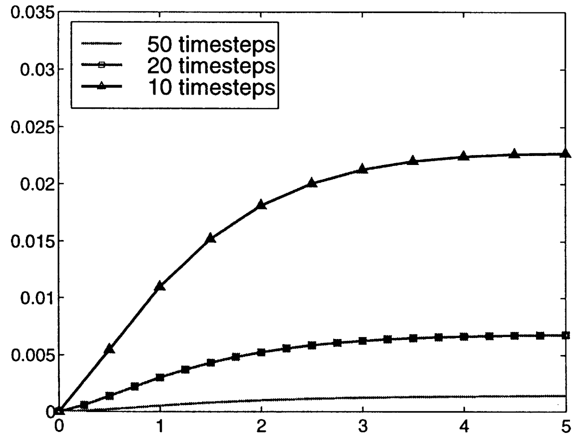

Fig. 10. Error due to non-coaxiality for the PRN-model with isotropic elasticity, associative flow rule and kinematic hardening. Influence of time discretization.

PRN-model, which is shown to be thermodynamically consistent but is conceptually flawed by the fact that the backstress is non-symmetrical. These properties are shared by the PDNSv-model, which was used for comparison. However, for small elastic strains the non-symmetry becomes negligible.

Numerical investigations carried out for the case of simple shear confirmed that the amount of plastic rotation is of no consequence for elastic isotropy. However, in the presence of elastic anisotropy the plastic rotation significantly affects the results (as expected). As to the issue of a "proper" implementation of the exponential backward Euler integration scheme in the presence of non-coaxiality (arising from anisotropy), the numerical results showed that it is important to account for this non-coaxiality in order to avoid excessive truncation errors. The classical algorithm for the logarithmic elastic law, which strongly resembles the small strain format, should thus be used with great care.

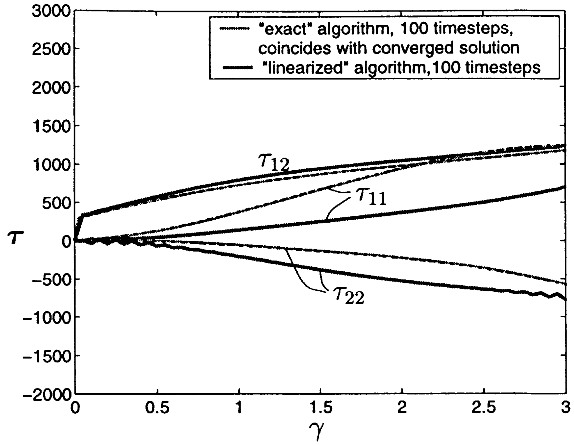

Fig. 11. In-plane stress τ components versus shear deformation γ for the PRN-model with transversely isotropic elasticity ($\theta = 90°$), associative flow rule and kinematic hardening. Influence of algorithm "linearization".

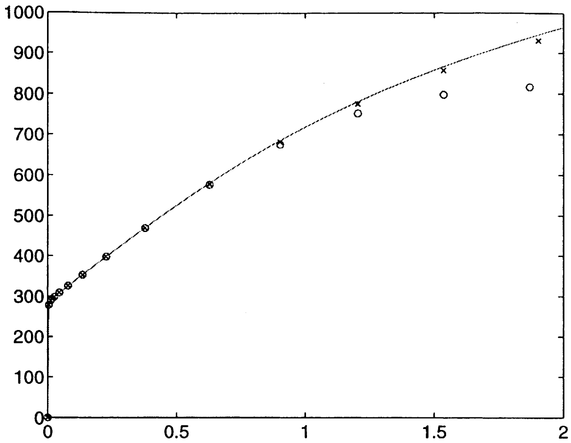

Fig. 12. Horizontal force versus displacement (of the top surface) for the unconstrained shear problem. Influence of algorithmic "linearization": exact (×), linearized (○), converged result (- - -).

Acknowledgements

We wish to acknowledge financial support from ABB Alstom Power, Volvo Aero Corporation and Volvo Aero Turbines, within the research project "Life prediction for thermomechanical loading of gas turbine components" coordinated by the Swedish Institute of Applied Mathematics (ITM).

References

Chaboche, J.L., Dang Van, K., Cordier, G., 1979. Modelization of the strain memory effect on cyclic hardening of 316 stainless steel. In Transactions of the Fifth International Conference on Structural Mechanics in Reactor Technology, Div. L, Berlin, L 11/3.

Eterovic, A.L., Bathe, K.L., 1990. A hyperelastic-based large strain elastoplastic constitutive formulation with combined isotropic-kinematic hardening using logarithmic stresses and strain measures. Int. J. Numer. Meth. Engng. 30, 1099–1115.

Lemaitre, J., Chaboche, J.L., 1990. Mechanics of Solid Materials. Cambridge University Press, Cambridge.

Münz, T., Runesson, K., Willam, K., 1999. Large strain plasticity analysis for kinematic hardening-an assessment of simple shear. Computational Mechanics, accepted for publication.

Perzyna, P., 1963. The constitutive equations for rate sensitive plastic materials. Q./q. Appl. Math. 20, 321.

Schieck, B., Stumpf, H., 1995. The appropiate corotational rate, exact formula for the plastic spin and constitutive model for finite elastoplasticity spin and constitutive model for finite elastoplasticity. Int. J. Solids Struct. 32 (24), 3643–3667.

Simo, J.C., 1988. A framework for finite strain elastoplasticity based on maximum plastic dissipation and the multiplicative decomposition: Part I. Continuum formulation. Comp. Meth. Appl. Mech. Engng. 66, 199–219.

Simo, J.C., Taylor, R.L., 1991. Quasi-incompressible finite elasticity in principle stretches-continuum basis and numerical algorithms. Comp. Meth. Appl. Mech. Engng. 85, 273–310.

Spencer, A.J.M., 1980. Continuum Mechanics. Longman, London.

Svendsen, B., Arndt, S., Klingbeil, D., Sievert, R., 1998. Hyperelastic models for elastoplasticity with non-linear isotropic and kinematic hardening at large deformation. Int. J. Solids Struct. 35, 3363–3389.

Tsakmakis, C., 1996. Kinematic hardening rules in finite plasticity, part i: a constitutive approach. Continuum Mech. Thermodynam. 8, 215–231.

Weber, G., Anand, L., 1990. Finite deformation constitutive equations and a time integration procedure for isotropic, hyperelastic–viscoplastic solid. Comp. Meth. Appl. Mech. Engng. 79 (2), 173–202.